Cellulose manuscript No.
(will be inserted by the editor)

Phase transitions of cellulose nanocrystal suspensions from nonlinear oscillatory shear

Supplementary information

Sylwia Wojno[1,2], Mina Fazilati[1,3,5], Tiina Nypelö[2,3], Gunnar Westman[2,4], Roland Kádár[1,2,*]

[1] Chalmers University of Technology, Department of Industrial and Materials Science, Division of Engineering Materials, SE-412 96 Gothenburg, Sweden

*Corresponding author: roland.kadar@chalmers.se

[2] Wallenberg Wood Science Centre (WWSC), Chalmers University of Technology, SE-412 96 Gothenburg

[3] Department of Chemistry and Chemical Engineering, Division of Applied Chemistry, Chalmers University of Technology, SE-412 96 Gothenburg

[4] Department of Chemistry and Chemical Engineering, Division of Chemistry and Biochemistry, Chalmers University of Technology, SE-412 96 Gothenburg

[5] Present address: Biofilms – Research Center for Biointerfaces, Faculty of Health and Society, Malmö University, SE-205 06 Malmö

Received: date / Revised version: date

Keywords Cellulose nanocrystals (CNCs), CNC water suspensions, self-assembly phases, rheology, birefringence, Fourier-transform rheology, stress decomposition

Zeta potential

The Zeta potential and particle size of CNC suspensions was measured using a Zetasizer Nano ZS (Malvern Instruments, UK) and DTS1070 folded capillary cells. A 50 mW diode-pumped solid-state laser was used as the light source with a wavelength of 532 nm. A CNC suspension of 0.1 wt% were analyzed in 10 mM NaCl, that was added to obtain an accurate zeta potential value such that the electrical double layer thickness around CNCs is not infinite leading to stronger chiral interaction between nano-rodlike particles (Qi et al. 2015; Reid et al. 2017). All measurements were conducted at 25 °C using stabilization time of 120 s, repeated 5 times and the average value was taken as final. The CNC particles in the presence of 0.1 mM NaCl salt showed an average zeta potential value -32.0 ± 3.4 mV, Tab. SS1. This indicates colloidal stability of the suspension at the macroscopic level. Values of > 30 mV have previously been reported to indicate highly stable CNC colloids in 0.1 mM NaCl (Bhattacharjee 2016; Patel and Agrawal 2011). In addition, similar values to the present determinations were obtained by Shafiei-Sabet et al. (2014).

The power-law model is expressed by the equation:

$$\eta(\dot{\gamma}) = K \cdot \dot{\gamma}^{n-1} \tag{S1}$$

where K is the consistency index and n is the flow index.

Table S1: Physico-chemical properties of CNC suspensions

Sample	ζ-potential [mV]	Conductivity [mS/cm]
1	-28.5	0.0128
2	-29.4	0.0247
3	-31.2	0.0129
4	-34.9	0.0169
5	-36.4	0.0171

Table S2: Power law flow indices (n), see equation (S1), at low $[10^{-3}, 10^{-1}]$ 1/s and high $[10^{0}, 10^{2}]$ shear rates for all non-siotropic concentrations.

CNC [wt%]	$\dot{\gamma} \in [10^{-3}, 10^{-1}]$	$\dot{\gamma} \in [10^{0}, 10^{2}]$
3	0.33	0.24
4	0.30	0.19
5	0.12	0.10
6	0.10	0.03
7	0.07	0.03
8	0.06	0.04
9	0.02	0.005

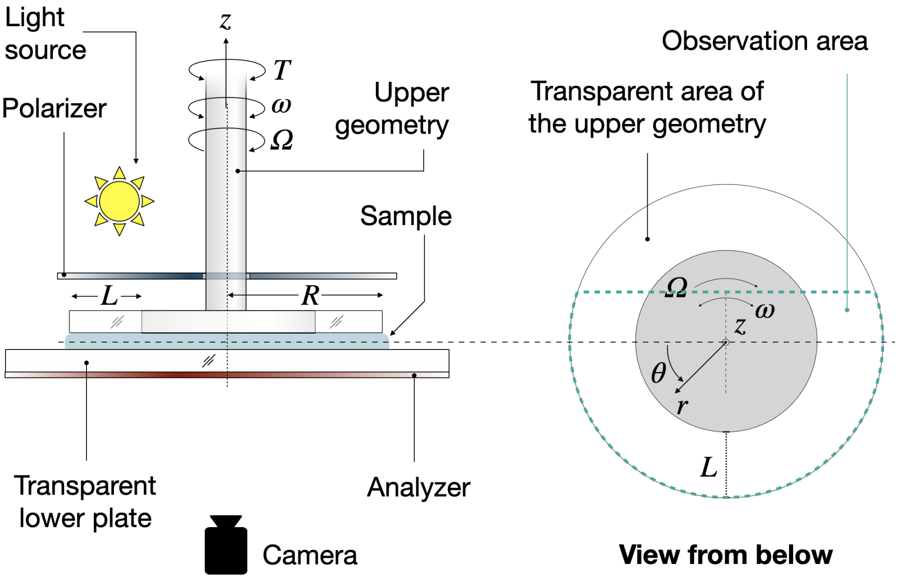

Fig. S1: Schematic overview of the combined rheology polarized light imaging (rheo-PLI) setup.

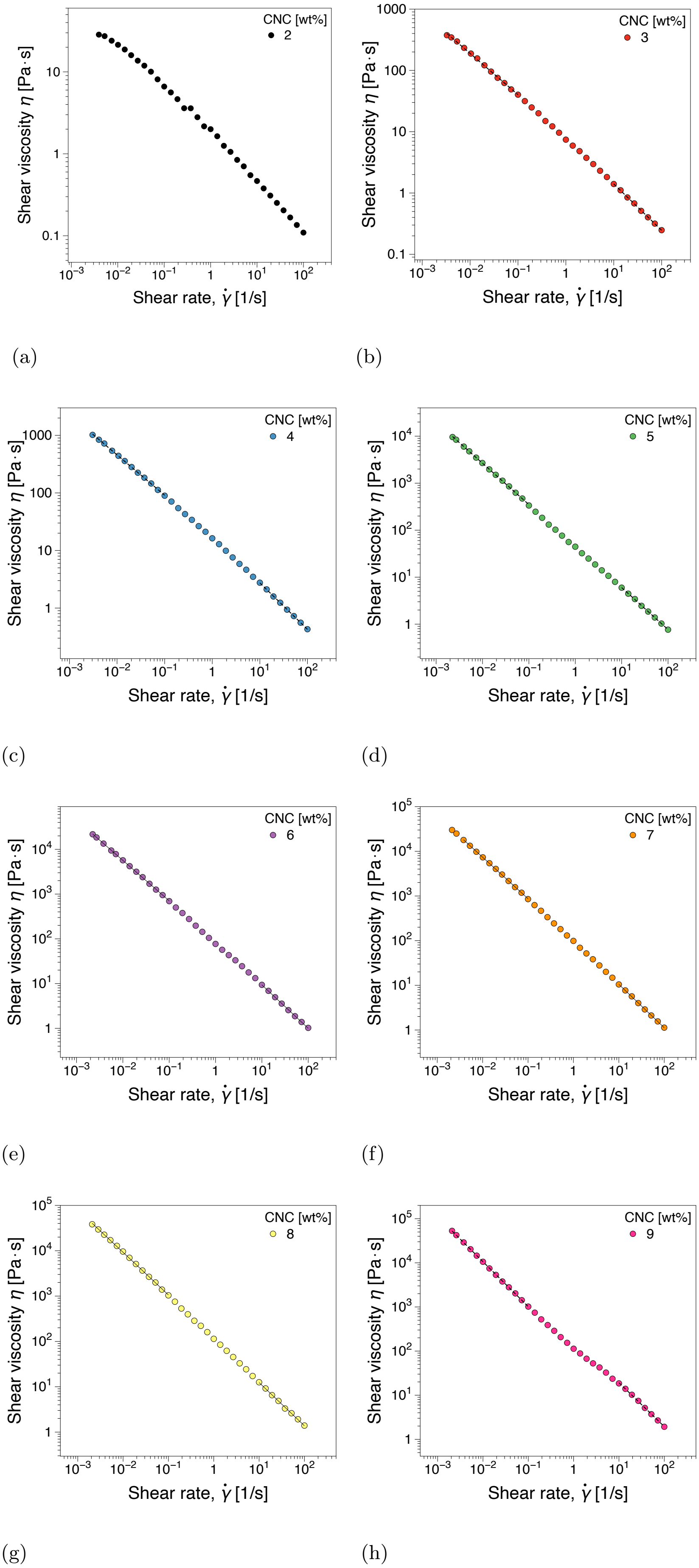

Fig. S2: Steady shear viscosity of the separated CNC suspensions.

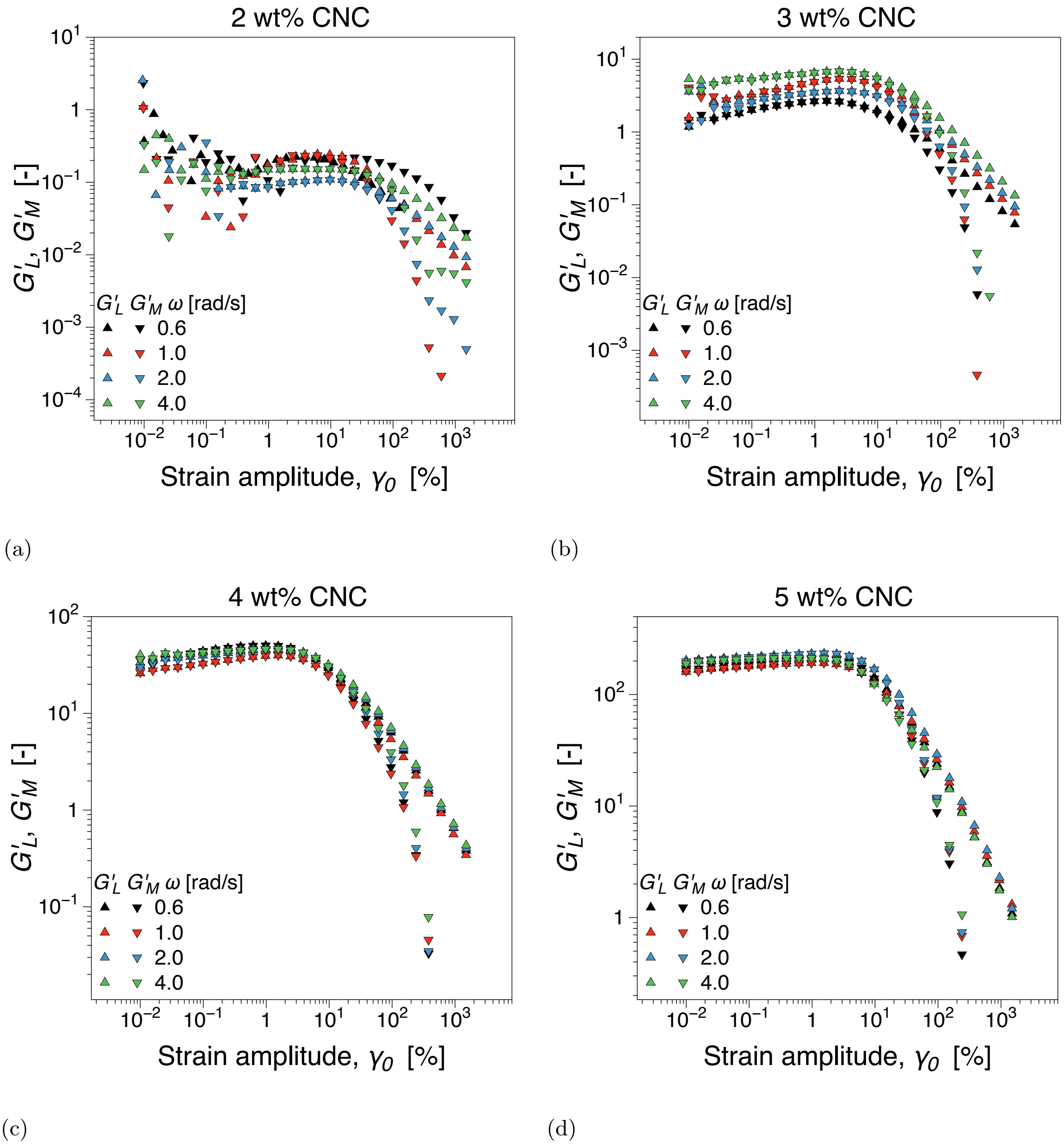

Fig. S3: Nonlinear viscoelastic parameters G'_L, G'_M for: (a) 2 wt%, (b) 3 wt%, (c) 4 wt%, (d) 5 wt%, (e) 6 wt% (f) 7 wt%, (g) 8 wt% (h) 9 wt% CNC.

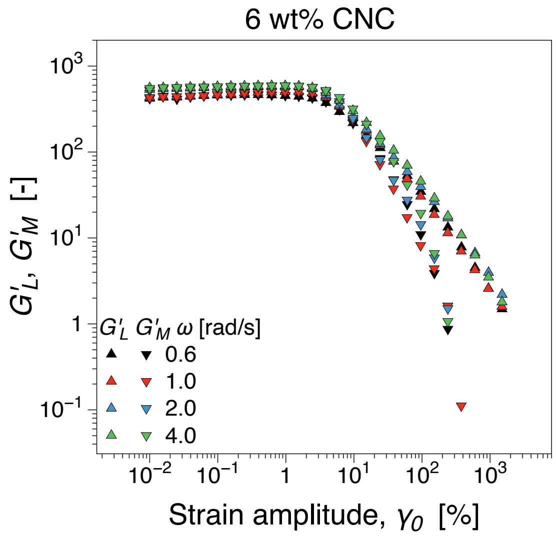

(a)

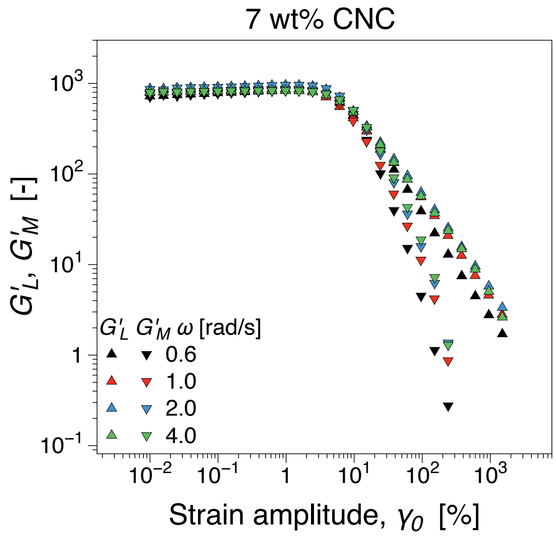

(b)

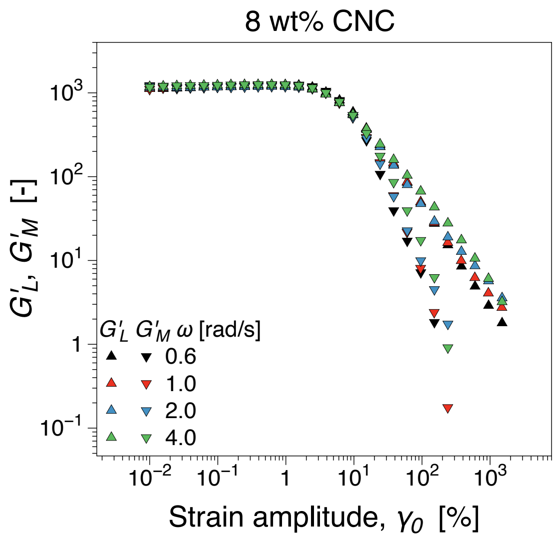

(c)

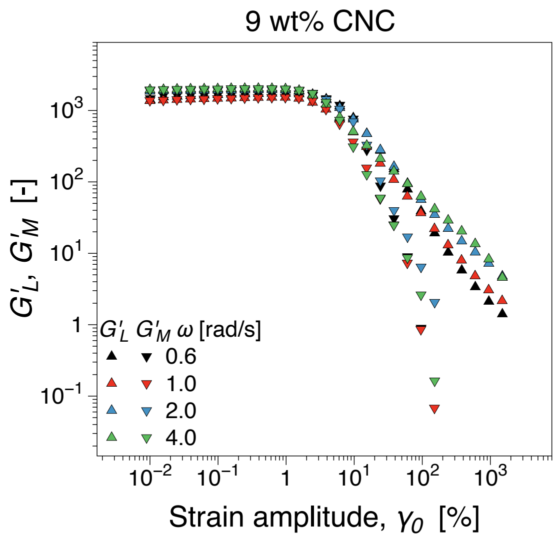

(d)

Fig. S3: (continued)

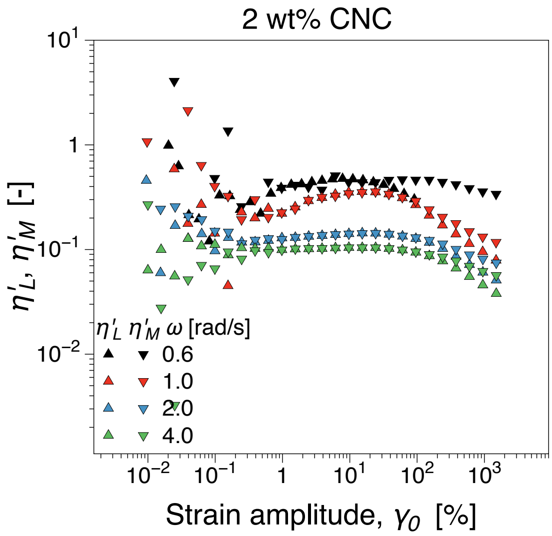

(a)

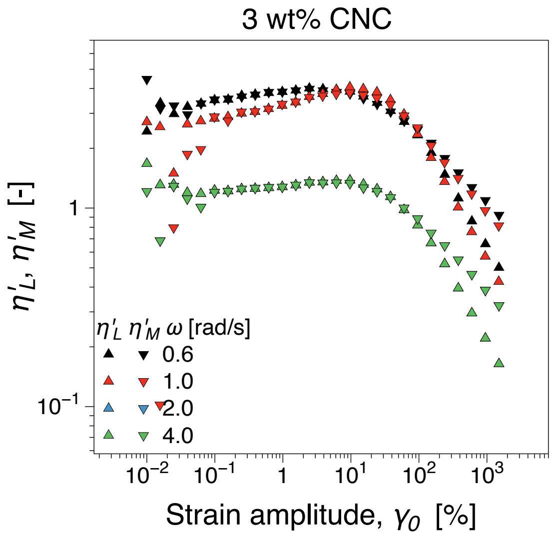

(b)

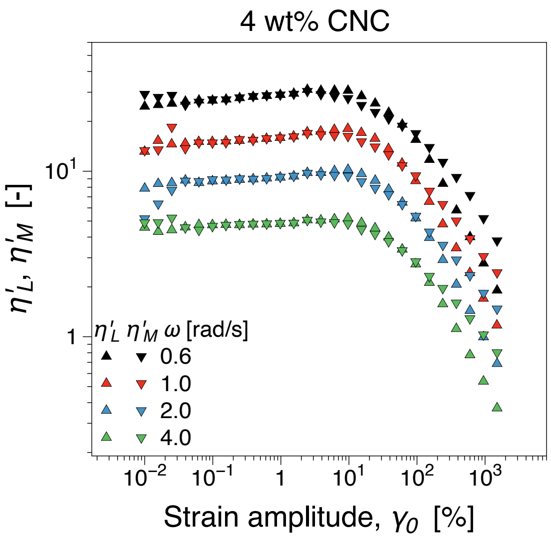

(c)

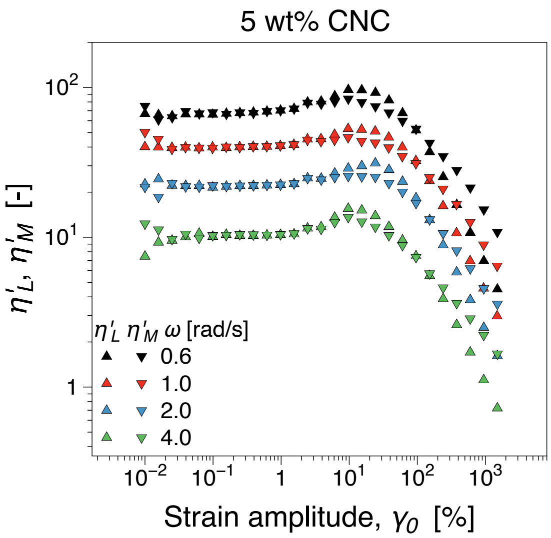

(d)

Fig. S4: Nonlinear viscoelastic parameters η'_L, η'_M for: (a) 2 wt%, (b) 3 wt%, (c) 4 wt%, (d) 5 wt%, (e) 6 wt% (f) 7 wt%, (g) 8 wt% (h) 9 wt% CNC.

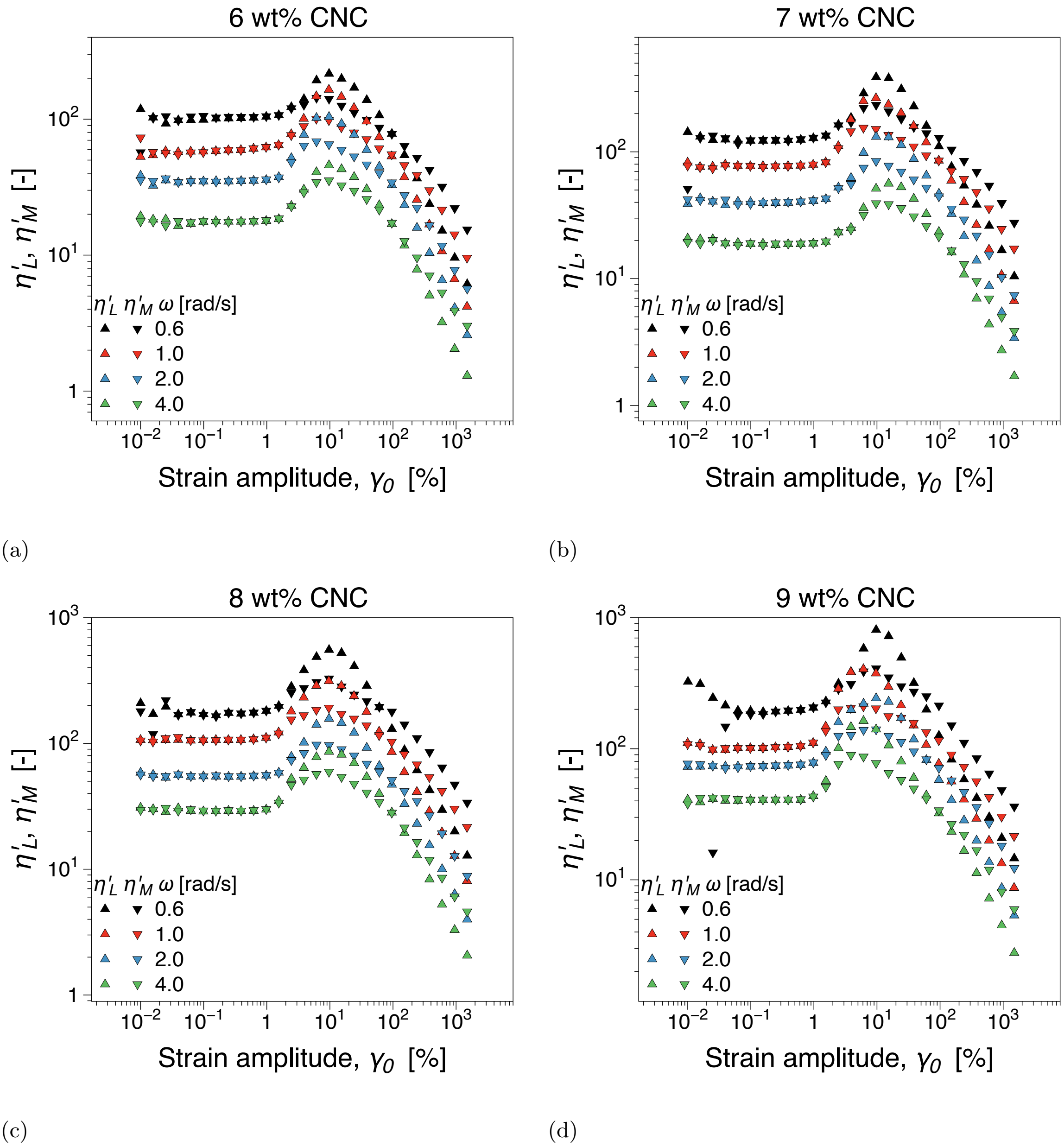

Fig. S4: (continued)

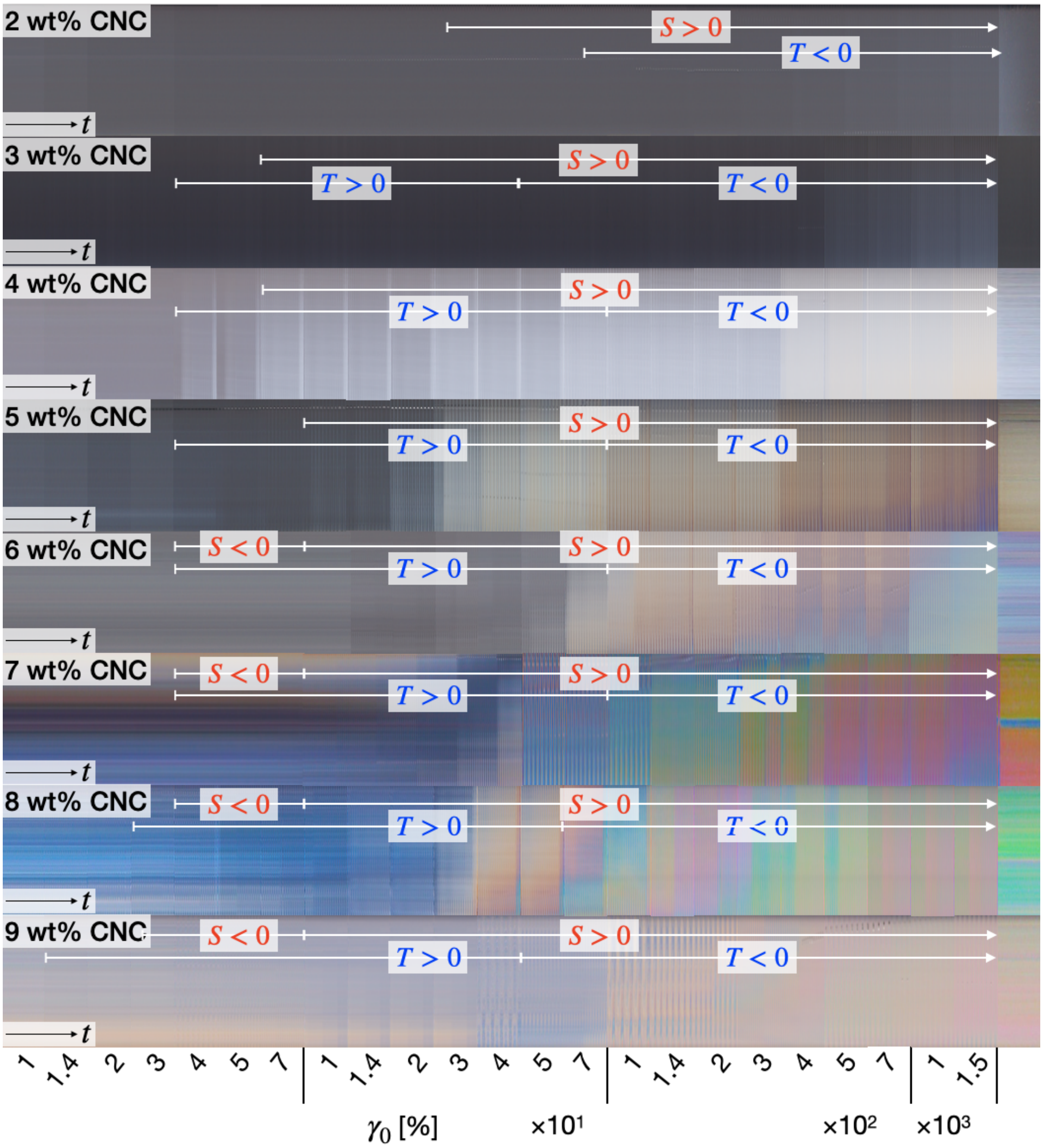

Fig. S5: Space-time optical visualizations of the birefringence pattern development and phase transition in strain sweep measurement at $\omega = 4$ rad/s.

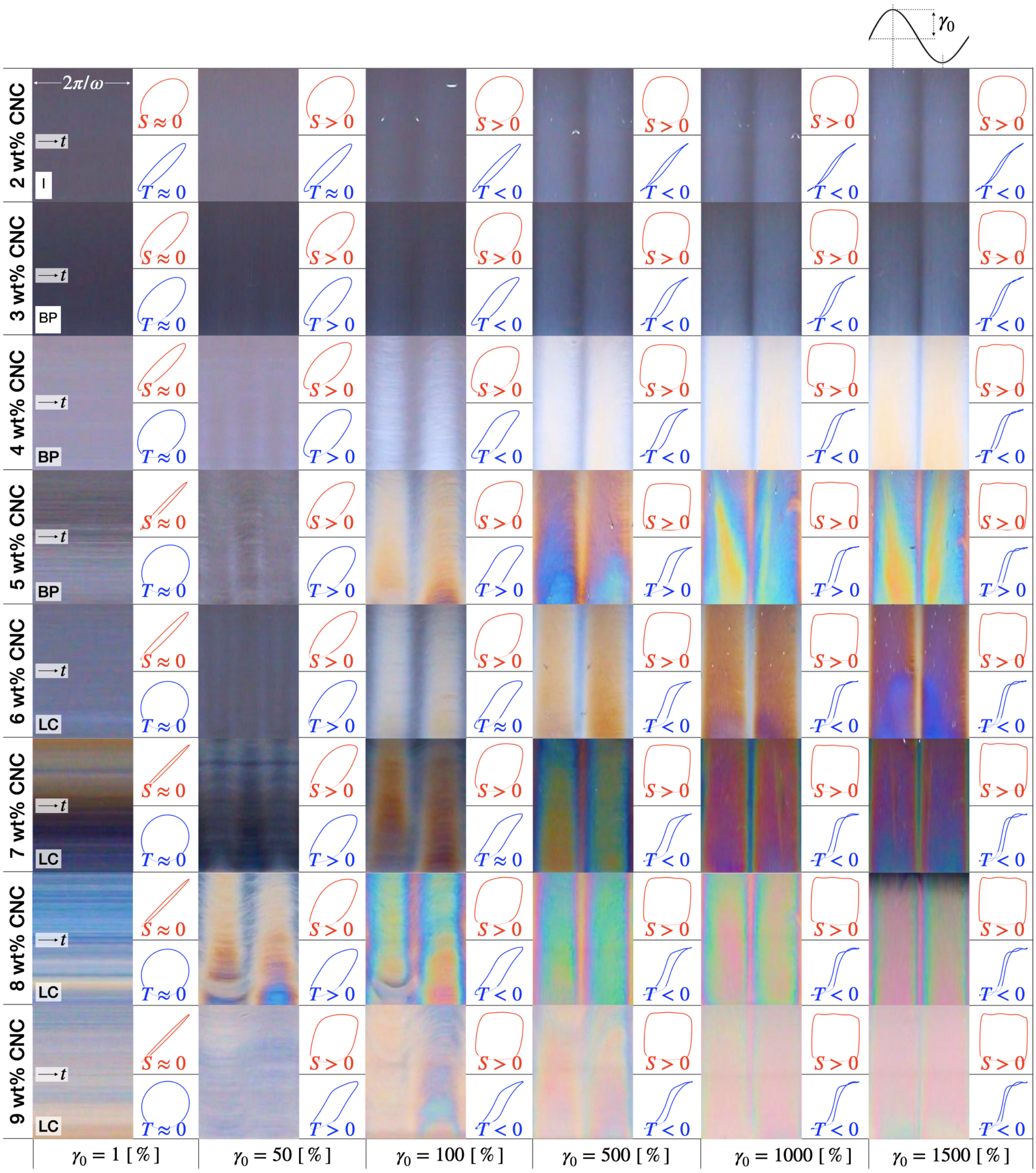

Fig. S6: Intra-cycle birefringence patterns strain amplitude for $\omega = 4$ rad/s, corresponding to the space-time diagrams in Fig.3 (SI).

Table S3: Comparative summary of nonlinear viscoelastic parameters development depending on a phase.

Phase	Isotropic (I)	Biphasic (BP)	Liquid crystalline (LC)
ϕ	2 wt%	3-5 wt%	6-9 wt%
$I_{3/1}$	$I_{3/1} \propto \gamma_0^{n<2}$ $I_{3/1} = I_{3/1}(\omega)$ $\omega = 0.6, 1\text{rad/s}$ i) $n \approx 1.8$ for $\gamma_0 \in [3, 9]$ % ii) $n \approx 0.5$ for $\gamma_0 \in [12, 60]$ % $\omega = 2$ rad/s i) $n \approx 2$ for $\gamma_0 \in [6, 23]$ % ii) $n \approx 0.85$ for $\gamma_0 \in [24, 95]$ % $\omega = 4$ rad/s $n \approx 1.9$ for $\gamma_0 \in [15, 95]$ %	3 wt% i) $n \approx 0.6$ for $\gamma_0 \in [1, 5]$ % ii) $n \approx 1.5$ for $\gamma_0 \in [5, 10]$ % 4 wt% i) $n \approx 1$ for $\gamma_0 \in [0.7, 3.8]$ % ii) $n \approx 1.6$ for $\gamma_0 \in [3.8, 10]$ % 5 wt% i) $n \approx 1.3$ for $\gamma_0 \in [0.95, 5]$ % ii) $n \approx 1.37$ for $\gamma_0 \in [5, 10]$ %	$n \approx 2$ for $\gamma_0 \in [1, 10]$ % $I_{3/1} = I_{3/1}(\omega)$
S	$S \approx 0$ for $\gamma_0 \in [0.01, 10]$ % $S > 0$ for $\gamma_0 \in [10, 1500]$ %		$S \approx 0$ for $\gamma_0 \in [0.01, 1.5]$ % $S < 0$ for $\gamma_0 \in [1.5, 10]$ % $S > 0$ for $\gamma_0 \in [10, 1500]$ %
T	$T \approx 0$ for $\gamma_0 \in [0.01, 15]$ % $T < 0$ for $\gamma_0 \in [15, 1500]$ %	$T \approx 0$ for $\gamma_0 \in [0.01, 3.8]$ % $T > 0$ for $\gamma_0 \in [3.8, 60]$ % $T < 0$ for $\gamma_0 \in [60, 1500]$ %	

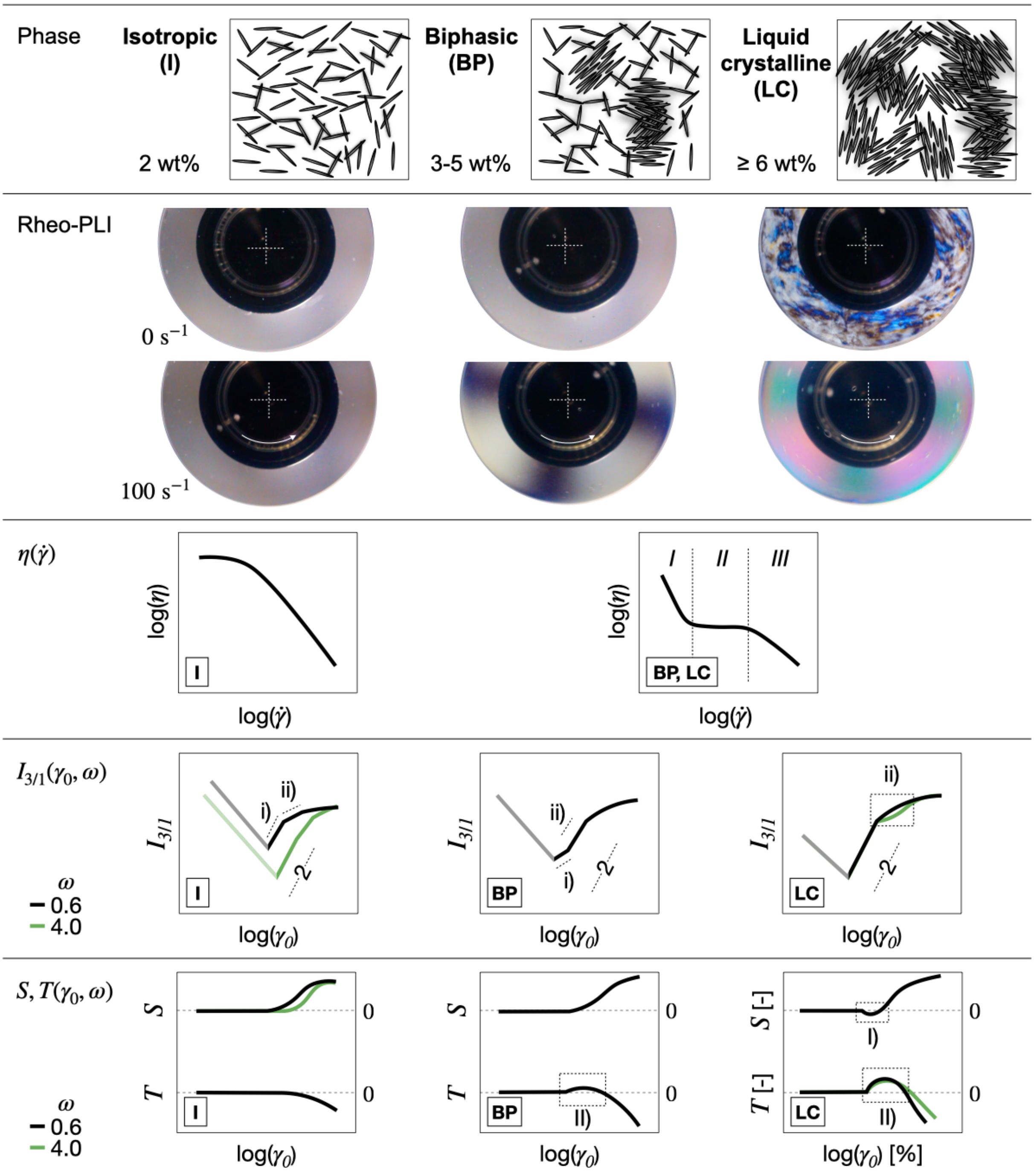

Fig. S7: Graphical summary of phase behavior as estimated based on PLI and rheological measurements with schematic illustrations and representative PLI.

References

Bhattacharjee, S. (2016). Dls and zeta potential –what they are and what they are not? *Journal of Controlled Release*, 235:337–351.

Patel, V. R. and Agrawal, Y. K. (2011). Nanosuspension: An approach to enhance solubility of drugs. *Journal of advanced pharmaceutical technology & research*, 2(2):81–82.

Qi, W., Xu, H.-N., and Zhang, L. (2015). The aggregation behavior of cellulose micro/nanoparticles in aqueous media. *RSC Adv*, 5:8770–8777.

Reid, M. S., Villalobos, M., and Cranston, E. D. (2017). Benchmarking cellulose nanocrystals: From the laboratory to industrial production. *Langmuir*, 33(7):1583–1598.

Shafiei-Sabet, S., Hamad, W. Y., and Hatzikiriakos, S. G. (2014). Ionic strength effects on the microstructure and shear rheology of cellulose nanocrystal suspensions. *Cellulose*, 21(5):3347–3359.